ORIGINAL INSTALLATION FOR COMPLEX MEASUREMENT OF ACOUSTIC PARAMETERS IN CONDENSED MEDIA

P.V. Bazylev, A.I. Kondratjev, V.A. Lugovoy
VNIIFTRI, Far Eastern Branch, Khabarovsk, Russia

Attenuation factor α_L and propagation velocity of longitudinal C_L and shear C_S ultrasonic (US) waves are the important informative parameters in US nondestructive testing materials and products. The accuracy and reliability of measurements of these physical quantities, metrological verification of acoustic measurements in solid media are pressing problems.

Reference installations of the immersion type for measuring the velocity of propagation and attenuation factor of US waves in metals (models IWA, UISU, ALPHA) do not meet modern requirements because of high measurement errors, and they are designed to measure only one parameter (α_L or C_L). Another disadvantage of the installations of this type is that, when measuring a systematic error component, they do not consider the influence of the liquid-solid interface peculiarities which are due to the surface gas adsorption [1]. Preliminary experiments and estimations have shown that the component of an error caused by surface adsorption decreases with the increase in the thickness of the sample. For samples of steel or aluminium alloys in the thickness of ~ 10 mm it can reach 20 m/s.

In the Far Eastern Branch of VNIIFTRI there has been developed an installation MAI-1 and approved as a working standard of 2-nd echelon (according to the State Verification System in conformity with Metrology Instructions MI 2055-90 and MI 2163-91). The list of measured parameters and the basic metrological characteristics of the installation are given in table 1. The installation operates in resonance and pulse-echo modes.

Table 1

The basic metrological characteristics of the installation MAI-1

Characteristic	Measurement range	Measurement error	Measurement uncertainty
Attenuation factor of longitudinal US waves	(0,2 ÷ 5) dB/m (5 ÷ 2000) dB/m	≤ 20 % ≤ 10 %	≤ 20 % ≤ 10 %
Velocity of longitudinal US wave propagation	(2000 ÷ 15000) m/s	≤ 0,05 %	≤ 0,05 %
Frequency range of US vibrations	(1 ÷ 100) MHz	±10 Hz	±10 Hz
Group velocity of shear US wave propagation	(1000 ÷ 7000) m/s	≤0,5 %	≤0,5 %

The installation embodies non-contact methods of generation and reception of US vibrations on the basis of capacitance transducers (CT) with thin-film oxide dielectric [2-4].

The main advantages of the installation are:

- Complex measurement of parameters of US wave propagation α_L, C_L, C_S;
- Use of non-contact methods of generation and reception of US waves eliminating the use of immersion liquids, and, thereby eliminating distortions of amplitude-phase characteristics of US pulses and loss of acoustic energy when passing through the liquid-solid interface, which reduces the systematic error component;
- Elimination of the necessity to readjust the radiator and the receiver in the full range of working frequencies for measurement.

The block diagram of the installation is shown in figure 1.

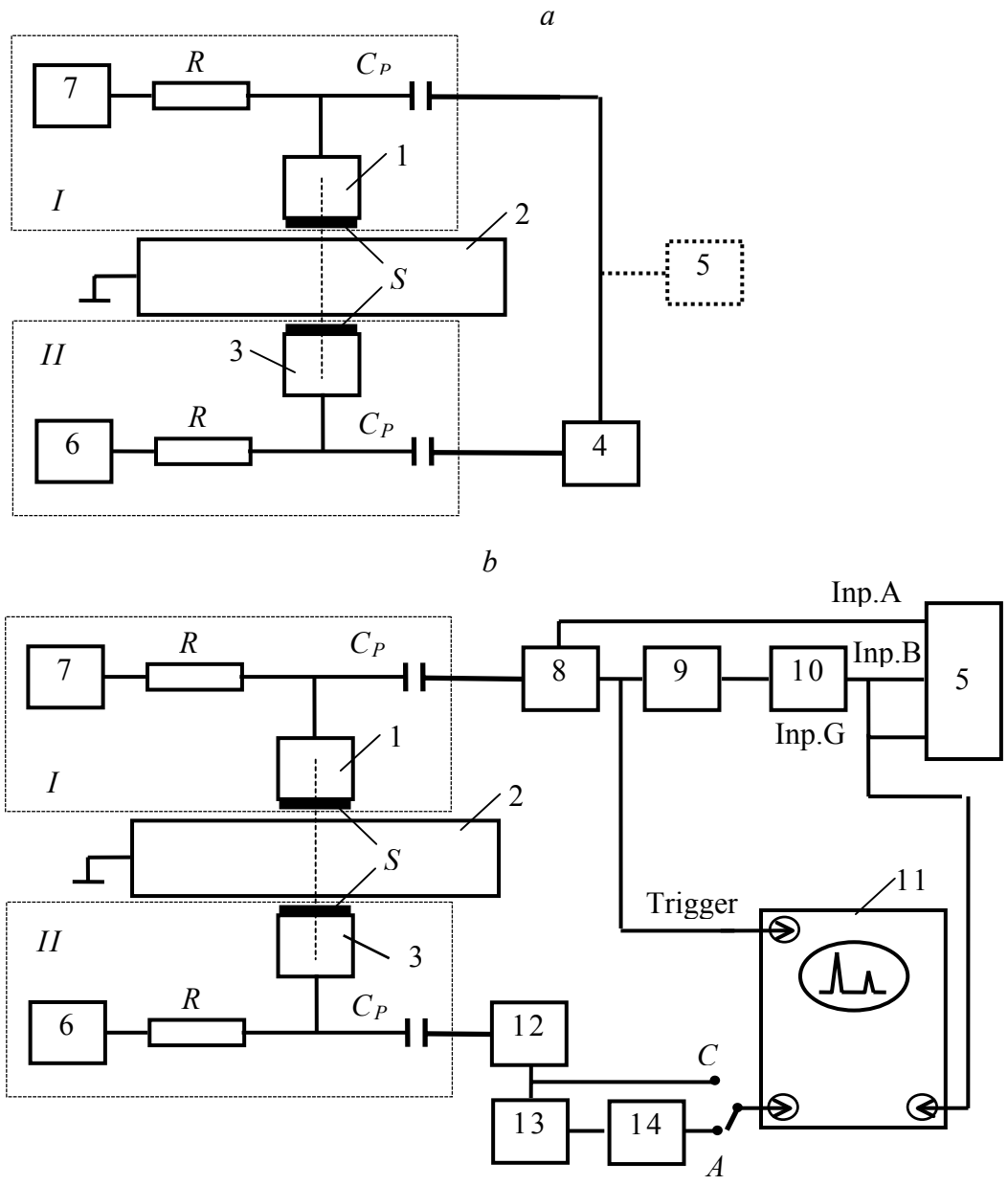

Fig. 1. Block diagram of the installation MAI-1 measuring parameters C_L and α by resonance (*a*) and pulse (*b*) methods: *I*, *II* - excitation and reception capacitance transducers; 1, 3 - electrodes; 2 - sample; 4 - spectrum analyzer; 5 - frequency meter; 6, 7 - sources of d.c. polarizing voltage; 8 - generator of radio pulses; 9 - generator of detained pulses; 10 - generator of doubled pulses; 11 - oscillograph; 12 - preamplifier; 13 - attenuator; 14 - band-pass amplifier with detector; 15 - attenuation measuring instrument; C_p - dividing capacity; *R* - charging resistance

In the resonance method, for the case of a plane wave, surface vibrations in a plane-parallel sample in thickness *d* are defined by a following equation [2]:

$$u = u_0 \frac{y \exp(j\psi)}{1 - y^2 \exp(2j\psi)}, \quad (1)$$

where u_0 is the amplitude of US vibrations; $y = \exp[-\alpha(\omega) d]$; $\psi = kd = \omega d/C_L$; $\omega = 2\pi f$; f is the fre-

quency of US vibrations.

Output signal of the reception transducer $U(\omega)$ and its phase $\varphi(\omega)$ may be given as

$$U(\omega)=K|u|=\frac{Ku_0 y}{\sqrt{1+y^4-2y^2\cos 2\psi}}; \tag{2}$$

$$\varphi(\omega)=\arg U(\omega)=\psi+arctg\left(\frac{y^2\sin 2\psi}{1-y^2\cos 2\psi}\right)+\varphi_0, \tag{3}$$

where K is the module of transformation factor of the of US vibration receiver; φ_0 is the phase shift in the transducer.

The maximum function (2) is reached when $\psi = \pi n$, and its minimum is reached when $\psi = \pi(n+1/2)$, where n =1,2,3... Which are the numbers of the acoustic spectral lines formed when the frequency of the setting generator changes.

$$U_{\max}=U_n=\frac{Ku_0 y}{1-y^2};\ U_{\min}=U_{n\pm 1/2}=\frac{Ku_0 y}{1+y^2} \tag{4}$$

At small values of the attenuation factor (y is close to 1) the width of an acoustic spectral line ΔF with the level of 0,707 is connected with α by a simple relation [2]

$$\alpha=\frac{20}{\ln 10}\frac{\pi(\Delta F-\Delta F_{POP})}{C_L},\ (\text{dB/m}) \tag{5}$$

where ΔF_{POP} is the correction including the loss of acoustic vibration energy into the environment.

The resulted expression has an error less than 0,5 % at $\Delta F \le 0{,}1\Delta f$, where Δf is a frequency interval between the neighboring spectral lines. In measuring ΔF at the level β from a maximum, for α the following is received:

$$\alpha=-\frac{20}{d}\lg\left[-\frac{\beta\sin\Delta\psi}{\sqrt{1-\beta^2}}+\sqrt{\left(\frac{\beta\sin\Delta\psi}{\sqrt{1-\beta^2}}\right)^2+1}\right], \tag{6}$$

where $\Delta\psi = \pi(\Delta F - \Delta F_{POP})/C_L$.

Expression (6) allows the definition α at $y \ge 0{,}01$. A random component of errors characterized by mean-square error (MSE) in equations (5) and (6) can be presented as

$$S_\alpha=\alpha\left[\left(\frac{S_F}{\Delta F}\right)^2+\left(\frac{S_f}{\Delta f}\right)^2\right]^{1/2}, \tag{7}$$

where S_F and S_f are the measurement errors of frequency intervals ΔF and Δf respectively.

According to expressions (4) α can also be defined by the following formula

$$\alpha=\frac{10}{d}\lg\left(\frac{U_n+U_{n\pm 1/2}}{U_n-U_{n\pm 1/2}}\right) \tag{8}$$

$$S_\alpha=\left[\left(\frac{\alpha}{d}S_d\right)^2+\left(\frac{20}{d\ln 10}\frac{S_U}{U_n+U_{n\pm 1/2}}\right)^2\right]^{1/2}, \tag{9}$$

where S_d and S_U are the errors of measurement of a sample thickness and a signal size respectively.

The range of a residual systematic error (RSE) resulting from the measurement of the attenuation factor in the installation MAI-1 are defined (at the confidence probability P=0,95) from the following

equation:

$$\theta_{\alpha F} = 1{,}1\left[\sum_{l=1}^{7}(\theta^{i}_{\alpha F})^2\right]^{1/2}, \qquad (10)$$

where $\theta^1_{\alpha F} \approx 20\pi\overline{\Delta F}\Delta C_L (C_L^2 \ln 10)^{-1} \le 8\cdot 10^{-6}\overline{\Delta F}$, dB/m is the RSE caused by the errors in measuring the velocity of US waves; $\theta^2_{\alpha F} \approx 0{,}2$ dB/m and $\theta^3_{\alpha F} \approx 0{,}1$ dB/m are the RSEs caused by misalignment and difference in diameters of excitation and reception CT (they are defined experimentally); $\theta^4_{\alpha F} \le 3{,}47\,(k_L a\varphi)/d$ is the RSE caused by the non-plane parallelism (angle φ) of the working surfaces of the samples (at $f \le 100$ MHz, $\varphi \le 1\cdot 10^{-6}$ radian $\theta^4_{\alpha F} \approx 0{,}1$ dB/m) [1]; $\theta^5_{\alpha F} \le k_T \delta T$ is the RSE caused by instability of the sample temperature, (at $k_T \le 1$ dB/(m·grade); $d \le 0{,}025$ m; $\delta T \le 0{,}1^0$C; $\theta^5_{\alpha F} \le 0{,}1$ dB/m); $\theta^6_{\alpha F} \approx 20\pi\delta F_{SH}(C_L \ln 10)^{-1}$ is the RSE caused by a surface roughness of the sample; $\theta^7_{\alpha F} \approx 20\pi\delta F_P (C_L \ln 10)^{-1}$ is the RSE caused by the loss of acoustic energy into the environment and into the installation elements.

In order to define the error components $\theta^6_{\alpha F}$ and $\theta^7_{\alpha F}$ the width of acoustic spectral lines also have been measured at various values of a surface roughness R_a and with the damping of the surface areas of the samples fabricated of different materials. In tables 2, 3 the results of measurements for the sample of alloy D16T with $d = 0{,}025$ m (S is the total damping area) are shown.

Table 2

Influence of the surface roughness on the results of measurements

R_a, microns	$\overline{\Delta F}$ (Hz) at frequency f (MHz)					
	2,0	5,0	10,0	15,1	25,0	50,0*
0,034	268±10	1315±10	2930±10	19350±100	30420±200	50090±400
0,140	270±10	1320±10	2970±10	19500±100	30600±200	51400±400
0,463	272±10	1329±10	3180±10	21040±100	31800±200	54510±400
0,742	277±10	1333±10	3330±10	20070±100	32620±200	58680±400

Table 3

Loss of acoustic energy into the environment (R_a = 0,14 microns)

S, мм^2	$\overline{\Delta F}$ (Hz) at frequency f (MHz)					
	1,0	2,0	2,9	5,1	15,1	50,0*
0	210±10	270±10	580±10	1320±10	19500±100	52400±400
16	270±10	330±10	610±10	1330±10	19700±100	52600±400
32	290±10	400±10	650±10	1370±10	19600±100	52800±400
48	340±10	400±10	700±10	1390±10	19900±100	52600±400
64	430±10	500±10	730±10	1400±10	20000±100	53000±400

* Measurements were made at level 0,9

The processing of the data in tables 2, 3 has shown that the error θ_{A6} can be approximated by the expression $\theta^6_{\alpha F} \approx 4 f^2 Ra$ dB/m (f is expressed in MHz and R_a in microns), and ΔF_{POP} may be given as

$$\Delta F_{POP} = \frac{1{,}8 \cdot 10^9}{\rho C_L (1 + 0{,}01 f^3)}, \tag{11}$$

where ρ is the density of the material of the sample in kg/m^3; f is the frequency of US vibrations in MHz.

The error in expression (11) at $f \le 10$ MHz does not exceed 20 Hz. In the range of frequencies above 10 MHz ΔF_{POP} <5 Hz.

From the preceding, the range of RSE and the error range resulting from the measurement of α by the resonance method may be shown as follows:

$$\theta_{\alpha F} \approx \left[0{,}03 + 2 \cdot 10^{-11} \left(\overline{\Delta F} \right)^2 \right]^{1/2};$$

$$\Delta \alpha_F \approx 2{,}11 \left[(S_\alpha)^2 + \frac{1}{3} (\theta_{\alpha F})^2 \right]^{1/2} \approx \left[0{,}06 + 1{,}6 \cdot 10^{-6} \overline{\Delta F} + 4 \cdot 10^{-9} \left(\overline{\Delta F} \right)^2 \right]^{1/2} \tag{12}$$

The relative error in measuring α at $Ra \le 0{,}14$ microns does not exceed 20 % at $0{,}2 \le \alpha \le 5$ dB/m and is less than 10 % at $5 \le \alpha \le 300$ dB/m, in the frequency range of (1÷100) MHz.

For the resonance method, velocity C_L and random component S_{CL} of an error are connected with a frequency interval Δf by acoustic spectral lines and are expressed as follows:

$$C_L = 2 \Delta f d = \frac{2d(f_m - f_n)}{m - n}, \tag{13.1}$$

$$C_L = \frac{2 d f_m}{m} = \frac{2 d f_n}{n} \tag{13.2}$$

$$S_{CL} = C_L \left[\left(\frac{S_f}{\Delta f} \right)^2 + \left(\frac{S_d}{d} \right)^2 \right]^{1/2}, \; S_{CL} = C_L \left[\left(\frac{S_f}{f} \right)^2 + \left(\frac{S_d}{d} \right)^2 \right]^{1/2} \tag{14}$$

where f_m, and f_n are the frequencies of acoustic spectral lines with numbers m and n respectively (figure 2).

RSE range resulting from measuring velocity C_L, for installation MAI-1, is defined by the following expression (at the confidential probability of P=0,95)

$$\theta_{CLF} = 1{,}1 \left[\sum_{l=1}^{4} (\theta^i_{LF})^2 \right]^{1/2}, \tag{15}$$

where $\theta^1_{LF} \approx \delta O^2 \Delta f / (m-n)/10d$ is the RSE caused by misalignment δO of excitation and reception CT (at $\delta O \le 0{,}0005$ m and $d \ge 0{,}01$ m $\theta^1_{LF} \le 0{,}5$ m/s); $\theta^2_{LF} \approx 3(\Delta f d)/(m\text{-}n)$ is the RSE caused by the non-plane parallelism (angle φ) of the working surfaces of the samples (at $\varphi \le 1 \cdot 10^{-6}$ radian is $\theta^2_{LF} \le 0{,}02$ m/s); $\theta^3_{LF} \approx k_{CT} \delta T$ is the RSE caused by the temperature instability in the sample (at $k_{CT} \le 2$ m/(s·grade), $d \le 0{,}05$ m, $\delta T \le 0{,}1^0$C is $\theta^3_{LF} \le 0{,}4$ m/s); θ^4_{LF} is the RSE caused by the diffraction effects (the correction is defined by the results of checking with the data of the installation of the highest accuracy IHA 39-A-86 for the measurement of velocity of longitudinal ultrasonic wave propagation, at $\alpha \le 100$ dB/m $\theta^4_{LF} \approx$ 1 m/s; at $100 \le \alpha \le 300$ dB/m $\theta^4_{LF} \approx 2$ m/s).

Error range resulting from the measurement of C_L is defined by the following expression (at the confidential probability of P=0,95)

$$(\Delta C)_L = 2{,}11\left[(S_{CL})^2 + \frac{1}{3}(\theta_{CLF})^2\right]^{1/2} \quad (16)$$

For the resonance method, error range resulting from the measurement of the velocity is: at $\alpha \le$ 100 dB/m $(\Delta C)_L \le 2$ m/s; at $100 \le \alpha \le 300$ dB/m $(\Delta C)_L \le 3$ m/s.

Uncertainty of measurements can be calculated by the following formulas:

$$u_A(x) = S(x)$$

$$u_B(x) = \Theta(x)/\sqrt{3}$$

$$u_C(x) = \left[S^2(x) + \Theta^2(x)/3\right]^{1/2}$$

$$U_P(x) \approx \Delta x$$

The diffraction phenomena and superposition of re-reflections from surfaces limiting the sample are most strongly shown in the frequency range below 5 MHz (fig. 2 *d*). The superposition results in occurrence of satellites which amplitudes can be higher than those of the basic signal. They differ in the form, which makes possible their identification. To account for the diffraction effects in the frequency range below 5 MHz when defining parameters ΔF and Δf, equation (2) is replaced by the following improved expression for the amplitude of the output signal of the reception transducer:

$$u(f) = u_0 \left| \sum_{n=1}^{\infty} y^{(2n-1)} D(a, f, n) \exp[j(2n-1)\Psi)] \right|, \quad (17)$$

where $D(a,f,n) = 1 - \left[\left(1 - \frac{\xi_n^2}{2(ka)^2}\right) J_0(\xi_i) + j\left(1 - \frac{\xi_n^2}{2(ka)^2} + \frac{\xi_n}{(ka)^2}\right) J_1(\xi_n)\right] \exp(-j\xi_n)$ is the function in which the diffraction divergence of US vibrations is taken into account [2]; $\xi_n = k\left[\sqrt{(2n-1)^2 d^2 + (2a)^2} - (2n-1)\right]/2$; $J_0(\xi)$ and $J_1(\xi)$ are Bessel functions of zero and first order respectively.

Expression (17) makes possible to achieve the claimed metrological characteristics when measuring the attenuation factor and propagation velocity of longitudinal US waves in frequency range below 5 MHz.

Characteristic patterns of acoustic spectral lines are resulted in figure 2.

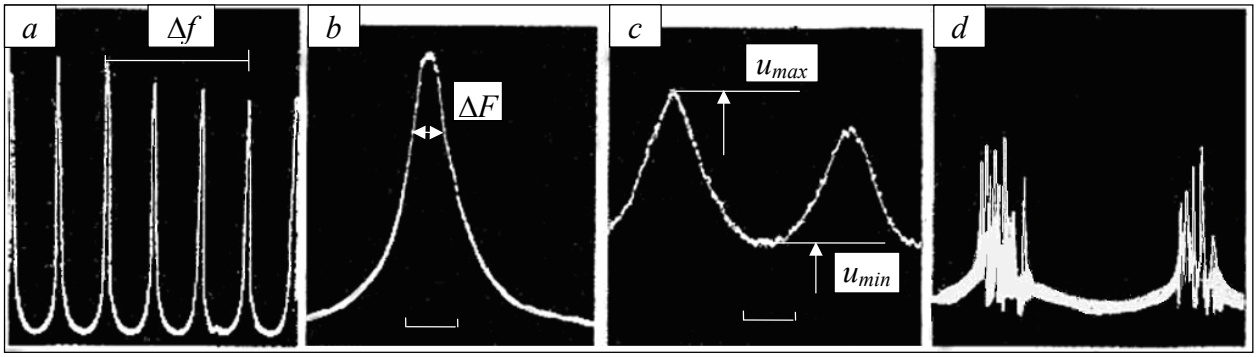

Fig. 2. Acoustic spectral lines: *a* - $f \approx$ 10 MHz, scan 0,2 MHz/div; *b* – $f \approx$ 9992,24 kHz, scan 5 kHz/div; *c* - $f \approx$ 15 MHz, scan 50 kHz/div (the sample steel X18H10T, d =15,00 mm); *d* - $f \approx$ 2,5 MHz, scan 20 kHz/div (the sample alloy D16T, d =25,00 mm)

In measuring by the resonance method (fig. 1 *a*) the installation works as follows. The signal from the output of the internal generator of the spectrum analyzer 4 of type СК4-59 moves to the input of excitation CT *I*. The ultrasonic vibrations of the sample 2 transformed by CT *II* into an electric signal, arrive at the input of СК4-59 on which screen the picture of acoustic spectral lines is seen (it can also be presented in a digital format). Power units 6 and 7, through the resistance (R ~1 MOhm), polarize CT *I* and CT *II* by d.c. voltage in the range up to 300 V. Electrodes 1 and 3 had the cylindrical form with diameters $2a$ from 1 to 20 mm and were made of aluminium alloy. Working surfaces of the electrodes were covered, by the anodizing method, with an oxide dielectric film in the thickness of ~10 microns.

Structurally, CTs are designed so that electrodes 1and 3 are pressed against the sample 2 without warps and with the constant effort ~ 1 N. For the samples, there are used the "plates" (non-plane parallelism of working surfaces is not more than $3 \cdot 10^{-5}$ radian), having the forms of a cylinder, a square, a parallelepiped, in thickness from 1 to 100 mm made of various materials (fused quartz, glass К8, steels 40Х13 and 12Х18Н10Т, alloy Д16Т, etc.). The working surfaces of dielectric samples have a sputtered metal layer (*Al*) in the thickness ~ 0,5 microns.

Measurements of the widths of acoustic spectral lines ΔF (fig. 2 *b*) and frequency intervals Δf (fig. 2 *a*) between them are made with the help of the internal frequency meter СК4-59, or by means of an external frequency meter 5 (a signal can be also presented and processed in a digital form). Values of propagation velocity and attenuation factor of US waves were calculated by formulas (5÷17). The choice of a formula to compute parameters α and C depended on the values of US wave attenuation in a single pass as well as on diffraction effects.

The characteristic pattern of the re-reflected US pulses, when the installation works in a pulse mode, is shown in figure 3.

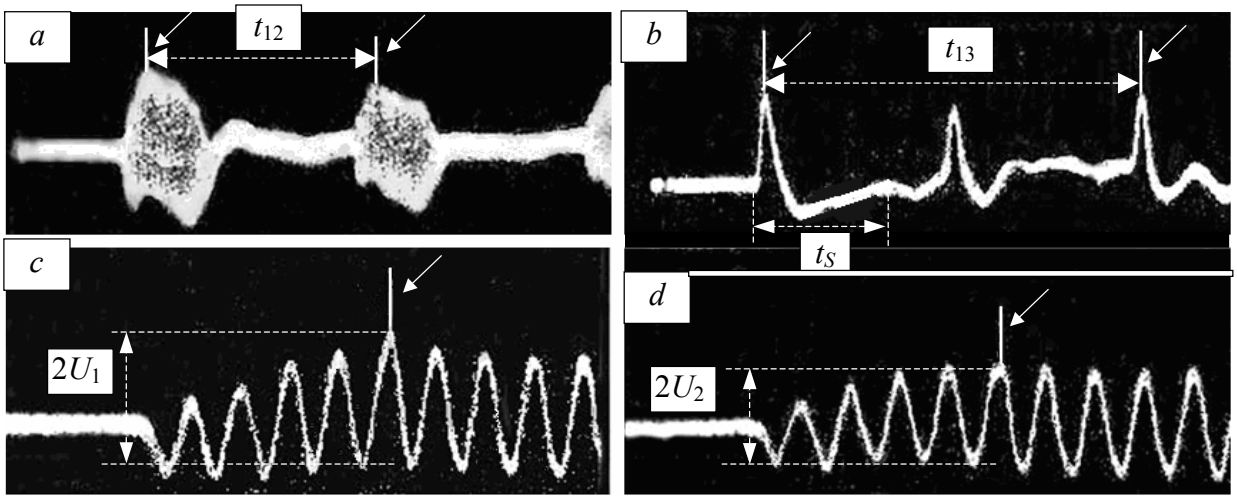

Fig. 3. Oscillograms of the re-reflected US pulses: *a* - radio pulse mode; *b* - "mono pulse" mode; *c* - the first US pulse; *d* - the second re-reflected US pulse; *a*, *b* - scan 1 μs/div; *c*, *d* - scan 0,1 μs/div.

The pulse method is used for the following: for parameter α, amplitudes U_n and U_m of chosen re-reflected pulses are measured (fig. 3 *c*, *d*); for parameter C_L and group velocity of longitudinal waves propagation C_{LG}, time intervals t_{nm} between them are measured; for the group velocity of shear waves propagation C_S, the time interval between the first incoming pulse of a longitudinal wave and a shear component of a signal t_S is measured (fig. 3 *b*). Measurements of C_{LG} and C_S are made in the "mo-

nopulse" mode (fig. 3 *b*). Values of propagation velocities and attenuation factor are calculated by the following formulas:

$$\alpha = \frac{A_{nm} - \Delta A_{DIF}}{2d(m-n)}, \tag{18}$$

$$\Delta A_{DIF} = 20\lg\left[\frac{|D(a,f,n)|}{|D(a,f,m)|}\right]; \tag{19}$$

$$C_L = \frac{2d}{(m-n)t_{nm}} + \Delta C_{DIF};\ C_{LG} = \frac{2d}{(m-n)t_{nm}}; \tag{20}$$

$$\Delta C_{DIF} = -\frac{2d}{(m-n)t_{nm}}\left[\frac{5{,}2}{z^{3/2}(k_l a)^2} + 7\cdot 10^{-4}\frac{(k_l a)^2 - 2200}{(k_l a)^2 + 13z^2}\right]; \tag{21}$$

$$C_S = \frac{C_{LG} d}{C_{LG} t_S + d} + (\Delta C_S)_{POP}; \tag{22}$$

$$(\Delta C_S)_{POP} = \frac{96}{z}\exp\left[-\left\{1{,}76\left(1 - \frac{z}{15}\right)\right\}^4\right], \tag{23}$$

where $A_{nm} = 20\lg(U_n/U_m)$ is the attenuation between numbers n and m of the re-reflected US pulses; ΔA_{DIF} is the diffraction correction in defining the attenuation factor; ΔC_{DIF} is the diffraction correction in defining the velocity; $(\Delta C_S)_{POP}$ is the correction considering the sizes of an electrode, and $z = d/a$. Corrections ΔC_{DIF} and $(\Delta C_S)_{POP}$ are defined based on the results of checking with the data of the installation of the highest accuracy IHA39-A-86. Values A_{nm} and ΔA_{DIF} are expressed in dB.

The time interval t_{nm} can be measured either by the autocorrelation method or by labels.

The factors which cause an error when measuring parameter α by the pulse method are the same as for the resonance method, but in the range of low frequencies the contribution of an error caused by the diffraction effects is larger. Experimental data processing with influencing factors and diffraction effects taken into account, resulted in the following expressions for mean-square error S_α and residual systematic error θ_α in measuring the attenuation factor by installation MAI-1 working in the pulse mode (requirements for the samples and temperature instability the same as for the resonance method):

$$S_\alpha \approx \frac{0{,}025(1+0{,}1A_{nm})}{2d(m-n)};\ \theta_\alpha = \frac{0{,}035}{2d(m-n)}, \text{ дБ/м} \tag{24}$$

where d is expressed in meters.

Error range resulting from measuring α is defined as follows:

$$\Delta\alpha_I \approx 2{,}11\left[(S_\alpha)^2 + \frac{1}{3}(\theta_\alpha)^2\right]^{1/2} \tag{25}$$

At $d \geq 0{,}01$ m and $f \geq 5$ MHz error α measured by pulse method is less than 10 % in the range of $10 \leq \alpha \leq 2000$ dB/m.

Error range resulting from measuring C_L, C_{LG} and C_S at the confidential probability P=0,95 is defined by the following:

$$(\Delta C)^{L,S} = 2{,}11\left[(S_{L,S})^2 + \frac{1}{3}(\theta_{L,S})^2\right], \tag{26}$$

where $S_L = C_L S_t / t_{nm}$; S_t is the MSE resulting from measuring the time interval t_{nm} for the velocity of longitudinal waves (for radio pulse and "monopulse" modes they coincide); $S_S = C_S S_{tS} / d$; S_{tS} is the

MSE resulting from measuring the time interval t_S for shear waves; θ_L and θ_S are the RSEs resulting from measuring the velocity of longitudinal and shear waves respectively.

Systematic components of errors resulting from measuring velocities C_L, C_{LG}, C_S at confidential probability P=0,95 are defined by the following expression:

$$\theta_{CL,LG,S} = 1{,}1\left[\sum_{l=1}^{5}(\theta^{i}_{L,LG,S})^2\right]^{1/2}, \qquad (27)$$

where $\theta^1_{L,LG}, \theta^2_{L,LG}, \theta^3_{L,LG}$ are the RSE components which are the same as in expression (15); $\theta^4_L \approx 2$ m/s is the error in defining the diffraction corrections for expression (26) (in the radio pulse mode at $10 \le d \le 20$ mm $\theta^4_L \approx 5$ m/s, at $d \ge 20$ mm $\theta^4_L \approx 2$ m/s); $\theta^4_{LG} \approx (2 + \Delta C_{DIS}/2)$ m/s is the error caused by the diffraction effects and sound dispersion ΔC_{DIS}; at $\Delta C_{DIS} \approx 5$ m/s $\theta^4_{LG} \approx 5$ m/s (it was defined based on the results of checking the data received by the resonance and radio pulse methods); $\theta^4_S \approx 5$ m/s is the error in defining the correction $(\Delta C_S)_{POP}$; $\theta^5_L \approx \theta^5_{LG} \approx C_L\theta_t / t_{nm}$ and $\theta^5_S \approx C^2_S\theta_t / d$ are the errors caused by RSE resulting from measuring time intervals θ_t. At $d \ge 20$ mm $\theta^5_L \approx \theta^5_{LG} \approx \theta^5_S \approx 0{,}3$ m/s.

With the pulse method (fig. 1 *b*) the installation works as follows. The signal with the amplitude up to 100 V and the duration of (2÷20) μs in the range of frequencies (1÷100) MHz arrives from radio pulse generator at the input of the excitation CT *I*. In the sample 2, re-reflected US pulses are transformed by CT *II* into the electric signal and, through the preamplifier 12 of the type U3-33, attenuator 13 of the type AD-30 and the band-pass amplifier with the detector 14 (the pass-band is 600 kHz, the range of reconstructed frequencies is (1÷100) MHz), come in one of the inputs of the digital oscillograph 11 of the LeCroy type. The measurement of the amplitudes of the chosen pair of the re-reflected pulses is made either by means of an attenuator, or by the signal swing, as it is shown in fig. 3 *c*, *d*. Then the attenuation of the signal A_{nm} is calculated by the formula (18), and the attenuation factor α is computed with the diffraction corrections (19) taken into account.

In the radio pulse mode, the measurement of velocity is made as follows.

1. Measurements by labels. The scan of the oscillograph 11 was chosen so that a sequence of the re-reflected US pulses (fig. 3, *a*) can be observed on the screen. Next, by regulating the delay of the generator 9 (fig. 1 *b*) and the time shift of the generator 10, the approximate time coincidence of the pulses of generator 9 with the chosen half wave of a registered signal is achieved (fig. 3 *a*). After that, the oscillograph is switched to the "B *delay*" operating mode, exact coincidence the pulses is achieved (fig. 3 *c, d*), and, with the use of the frequency meter 5 (fig. 1), the time interval t_{nm} is defined (time interval can be measured with the use of interior labels of an oscillograph 11). Then the parameter C_L is computed by the formula (20) considering the diffraction correction (21).

2. Autocorrelation method. The time form of signal $U(t)$ is recorded. The re-reflected pulses (with numbers n and m) are chosen and autocorrelation function $S(\tau)$ is defined when τ changes from $t_{1n} = t_{nm} - 0{,}5$ μs to $t_{2n} = t_{nm} + t_U - 0{,}5$ μs with the step of 0,5 nanoseconds (t_{nm} is a time interval between the pulses defined "visually" with the margin error ≤ 0,2 μs; t_U is a pulse duration).

$$S(\tau) = \int_{t_{1n}}^{t_{2n}} U(t)U(t-\tau)dt \qquad (28)$$

Finally, the improved value of the time interval t_{nm} is defined by the maximum of function $S(\tau)$ and the velocity of longitudinal US waves is calculated. It should be noted that mean-square error of measuring result for the autocorrelation method is less than for the method of "labels", but the data processing takes more time.

In some cases there is no necessity to measure frequency dependence of US wave velocity and it

would be sufficient to know the average frequency for group velocity C_{LG} (in the absence of dispersion $C_{LG} = C_L$). In this case the measurement technique becomes significantly simpler; the installation is switched to the "the monopulse" operating mode. The scheme includes a standard G5-63 pulse generator instead of the radio pulse generator 8 (fig. 1). Duration of exciting pulses is established in the range of $(1 \cdot 10^{-7} \pm 2 \cdot 10^{-8})$ s. In this case a series of the re-reflected pulses is seen on the oscillograph screen (fig. 3 *b*). Further measurements are made by the above described ways, either by labels or by autocorrelation method.

When the velocity of shear wave propagation is measured, the installation works in the "monopulse" operating mode. At the first stage the measurement of velocity C_{LG} is made, then the method of "labels" is used to measure the time interval between the first incoming longitudinal pulse and a shear component of the signal (fig. 3 *b*). Occurrence of a shear component is caused by the fact that the sizes of the ultrasonic wave radiator are limited (in the case of a plane wave a shear component is absent). Calculations of the value of parameter C_S are made according to the formula (22) considering the corrections (23). To decrease the error of parameter C_S to 5 m/s, it would be appropriate to use transducers with the diameters of the working surface of ~ 2÷3 mm.

In tables 4, 5 the results of measurements for parameters C_L, C_{LG}, C_S received by resonance and pulse methods for various materials are shown.

Table 4

Comparative data resulting from the measurements for parameters C_L and α by the resonance (R) and pulse (I) methods for various frequencies

f, MHz		Glass K8 *d* = 20,00 mm		Steel 40X13 *d* = 20,93 mm		Alloy D16T *d* = 9,68 mm		Steel X18H10T *d* = 15,00 mm	
		C_L, m/s	α, dB/m	C_L, m/s	α, dB/m	C_L, m/s	α, dB/m	C_L, m/s	α, dB/m
1	R	5968±1	1,0±0,06	6003±1	0,52± 0,06	6397±2	1,8±0,2	5751±1	0,74± 0,06
	I	5970±5	2,5±2	6002±5	3±2	6400±5	4±2	5755±5	3±2
5	R	5969±1	6,9±0,1	5998±1	2,8±0,1	6395±2	6,9±0,2	5750±1	4,3±0,1
	I	5969±3	7±1	6000±3	4±1	6399±5	7±1	5757±3	5,5±1
10	R	5671±1	8,8±0,3	5996±1	9,4±0,3	6397±2	13,3±0,3	5745±1	21±1
	I	5969±3	9±1	5999±3	10±1	6399±5	12±1	5757±3	22±2
25	R	5969±1	59±2	5995±1	119±10	6395±2	89,4±3	5763±10	610±50
	I	5971±3	62±5	6000±3	125±10	6393±5	89±7	5761±10	620±50
50	R	5970±1	119±10	5997±2	343±30	6390±10	410±20	-	-
	I	5970±3	115±10	6003±5	350±30	6390±10	400±30	5750±20	2300± 200
100	R	5970±1	167±10	-	-	6380±20	620±60	-	-
	I	5972±3	170±10	6010±20	2080± 200	6385±10	640±60	-	-

Table 5

Results of measurements for parameters C_{LG} and C_S

Material	d, mm	C_{S0}, m/s*	C_S, m/s	C_{LG}, m/s*	C_{LG}, m/s
Quartz of mark КВ	25,00	3711±1	3711±10	5959±0,3	5961±5
Glass К8	20,00	3513±1	3506±11	5869±0,3	5970±5
Alloy Д16Т	9,68	3098±1	3095±11	6417,5±0,5	6414±6
	25,00	3098±1	3104±11	6417,3±0,5	6411±6
	50,05	3098±1	3089±11	6417,4±0,5	6410±6
Steel Х18Н10Т	15,0	3137±1	3134±11	5755,9±0,5	5758±6
	25,0	3137±1	3133±11	5755,5±0,5	5756±6
	30,0	3137±1	3135±11	5755,5±0,5	5753±6
Brass L63	10,02	2206±2	2222±11	4504,6±1	4506±6
	25,02	2206±2	2213±11	4505,2±1	4509±6
Steel 40Х13	10,01	3273±1	3278±11	6003,2±0,3	6003±5
	20,93	3273±1	3262±11	6002,9±0,3	6003±5
Steel 3	20,10	3001±1	2995±11	5917,4±0,5	5922±6

* Given measuring results were received by the installation of the highest accuracy IHA 39-A-86

From the above tables it is clear that within the error range the results for all methods coincide.

In order to check and adjust the means of the nondestructive ultrasonic testing it is necessary to fabricate standard samples. For the maintenance of the control reliability it is very important that the samples meet requirement of quality standard, the uniformity of their acoustic properties, in the cross-section of the sample in particular. Traditional contact methods do not always provide the necessary accuracy of the control of these properties. The installation MAI-1 meets these requirements.

Figure 4 presents the re-reflected US pulses received in one sample when the radiating and reception CTs are displaced about the axis of the sample by the distance r. The same figure shows clearly the presence of the heterogeneity in the test sample.

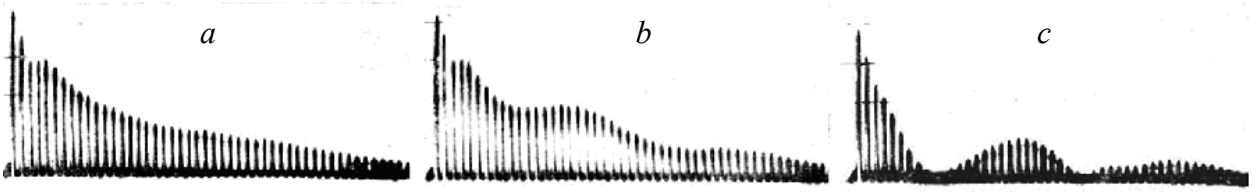

Fig. 4. Characteristic patterns of the re-reflected pulses. The sample of steel X18H10T, d =30 mm: a - r = 0; b - r = 10 mm; c - r = 40 mm.

Let us estimate a signal change at the output of the reception CT caused by the heterogeneity. For simplicity we will assume that, first, the working surface of an electrode has the form of a square with the side 2a and, second, attenuation factor α and wave number k in proximity to the point in the sample with co-ordinates (x_0, y_0) can be presented as follows [5]:

$$\alpha(x,y)=\alpha(x_0,y_0)+c_1(x-x_0)+c_2(y-y_0);\ k(x,y)=k(x_0,y_0)+c_3(x-x_0)+c_4(y-y_0);$$

$$c_1 \approx \left(\frac{d\alpha}{dx}\right)\Bigg|x = x_0 ; c_1 \approx \left(\frac{d\alpha}{dy}\right)\Bigg|y = y_0 ; \; c_3 \approx \frac{k(x_0, y_0)}{C_L}\left(\frac{dC_L}{dx}\right)\Bigg|x = x_0, y = y_0 ;$$

$$c_4 \approx \frac{k(x_0, y_0)}{C_L}\left(\frac{C_L}{d—}\right)\Bigg|x = x_0, y = y_0$$

Thus, the output signal of the reception CT for the US pulse which has passed a way z, is defined from the relation

$$u(x_0, y_0) = \frac{u_0}{4a^2}\int_{x_0-a}^{x_0+a} dx \int_{y_0-a}^{y_0+a} \exp\{[-\alpha(x_0, y_0) + jk(x_0, y_0)]z - [c_1(x - x_0) + c_2(y - y_0) - j(c_3(x - x_0) + c_4(y - y_0))]z\} dy =$$

$$\frac{u_0}{a^2}\exp\{[-\alpha(x_0, y_0) + jk(x_0, y_0)]z\}\left[\frac{-\mathrm{sh}(c_1 az)\cos(c_3 az) + j\mathrm{ch}(c_1 az)\sin(c_3 az)}{(-c_1 + jc_3)z}\right] \times$$

$$\left[\frac{-\mathrm{sh}(c_2 az)\cos(c_4 az) + j\mathrm{ch}(c_2 az)\sin(c_4 az)}{(-c_2 + jc_4)z}\right], \qquad (28)$$

where u_0 is a constant defined by the CT transformation coefficient and the amplitude of the US pulse.

From the relation (28) we can see that at $c_i az \ll 1$ signal in each point is defined only by the attenuation factor α and by the velocity C_L; at $c_3 az$, $c_4 az > 1$ the pattern of the re-reflected US pulses can have the oscillating character (fig. 4 *b, c*). At $c_i \neq 0$ and when az increases acoustic heterogeneity in re-reflected US pulses manifests more strongly.

In experiments, az was chosen so that the conditions $c_i az < 0{,}4$ were satisfied. In such cases definition errors α and C_L do not exceed the following values: $\delta\alpha / \alpha \approx (c_i az)^4 / 8 \approx 0{,}003$; $\delta C_L / C_L \approx (c_i az)^4 C_L / (2\pi f z) \approx 0{,}0002$.

Measurements were made as follows. The installation was shifted the radio pulse mode. Geometrical axes of the sample and capacitance transducers were made coincident ($r = \sqrt{x_0^2 + y_0^2} = 0$), and the frequency of US vibrations was selected in such a way as to decrease the manifestation of the diffraction effects. The screen of the oscillograph 11 shows the re-reflected pulses (fig. 4 *a*). Labels of an attenuation measuring instrument 15 are established according to the chosen pulses and the sample starts to move smoothly in a certain direction. Depending on the properties of the sample there can be three situations: in the first situation, a pattern of the re-reflected pulses and the indication of the attenuation measuring instrument do not change, i.e. the sample is acoustically homogeneous; in the second one, the monotonous character of pulse amplitude reduction remains, but attenuation changes; the third situation illustrates the changes in the pattern of re-reflected pulses according to fig. 4, *b* or fig. 4, *c*. In the second case, changes of the velocity are insignificant, and the sample is heterogeneous only in parameter α, in the third case it is heterogeneous both in velocity and attenuation. Then the sample is moved in such a way as to test it throughout.

Quantitative characteristics of heterogeneity were estimated by the attenuation factor.

In zero position when the axes of the CT and the sample coincide, parameter α_0 is measured. Then the attenuation, for example, between the first and fifth pulses is measured. Here the attenuation $A_{0\,\mathrm{is}}$ defined, it is expressed as $A_0 = 8d\alpha_0 + \Delta A_{\mathrm{DIF}}$.

When the sample is displaced by the distance r about the axis of CT and through the angle $\varphi = arctg(y/x)$ from any zero line, the attenuation may be written as $A(r, \phi) = 8d\alpha(r, \phi) + \Delta A_{\mathrm{DIF}}$. As-

suming that the change in the speed is insignificant and ΔA_{DIF} does not change, for $\Delta\alpha$ we receive

$$\Delta\alpha = \alpha_0 - \alpha(r,\phi) = \frac{A_0 - A(r,\phi)}{8d} \tag{29}$$

Attenuation sensitivity is $S_A \approx 0{,}022\ (1+0{,}1A)$ in dB. Minimum detected change in the attenuation factor can be estimated from the formula:

$$\Delta\alpha_{\min} = \frac{S_A}{8d} \approx \frac{0{,}022(1+0{,}1A)\cdot 10^{-2}}{8d},\ \text{dB/m}$$

where d is expressed in meters.

If the pattern of the re-reflected pulses is similar to fig. 4, *b*, *c*, according to expression (28), it is possible to receive the following equation for changes in velocity (assuming that the velocity depends only on x):

$$\Delta C \approx \frac{x{C_0}^2}{2 f z_{\min}}, \tag{30}$$

where C_0 is the value of velocity measured on an axis of the sample; $z_{\min}$ is the distance in which the first minimum of the re-reflected US pulse envelope is observed.

When the re-reflection pattern in the displaced sample changes slightly, to define ΔC the installation is shifted to the resonance mode and measurements are made in accordance with the position of displaced spectral lines. In zero position the spectrum analyzer CK4-59 is adjusted to a spectral line f_m, frequency intervals between lines f_{m-1} and f_{m+1} are measured, and zero value of velocity is computed as $C_0 = d\,(f_{m-1} - f_{m+1})$.

Then the sample is displaced and in this process the frequency of a spectral line m must be constantly observed. If the frequency of the lines has changed and has become equal to $f_m\,(r,\ \varphi)$, such velocity changes at this point may be presented as follows:

$$\Delta C = C_0 - C(r,\phi) = \frac{[f_m - f_m(r,\phi)]2d}{m}$$

Resolution of CK4-59 is10 Hz, and the minimum of detected velocity change is $\Delta C_{\min} \approx 4/m$, m/s (at $f \geq 5$ MHz, $\Delta C_{\min} \leq 0{,}01$m/c).

Measured results are illustrated in table 6.

Table 6

Acoustic heterogeneity of materials

№	Material of the sample	D, mm	d, mm	f, MHz	r, mm	C_0, m/s	ΔC, m/s	α_0 dB/m	$\Delta\alpha$, dB/m
1	Steel 3 [1]	100	20	5,0 10,0	15 15	5911 5911	1,5 0,1	41,3 261	0,7 33
2	Steel 45 [1]	50	10	5,0 30,0	10 10	5902 5903	0,2 -0,5	2,7 51,8	0,2 1,9
3	Steel 40X13 [1]	100	25	5,0 20,0	15 15	5940 5942	-1,6 -2,3	44,6 216	22 120
4	Steel 40X13 [4]	100	25	5,0 20,0	15 15	5938 5941	-1,0 -1,1	40,3 208	6 11
5	Steel 40X13 [3]	100	25	5,0 20,0	15 15	5927 5927	0,1 0,09	3,2 64,1	-0,2 0,6
6	Steel X18H10T [1]	120	25	5,0 10,0	15 15	5732 5728	0,1 -0,9	11,8 102	-3,1 28

7	Steel X18H10T [4]	120	25	5,0 10,0	15 15	5730 5729	0,1 -0,4	10,5 98,2	-2,5 18
8	Steel X18H10T [1]	100	30	5,0 10,0	15 15	5742 5740	0,7 -10	4,7 33,1	-0,8 -4,3
9	Brass L63 [1]	120	25	2,0 5,0	15 15	4429 4430	2,5 -0,3	28,1 168	-5 14
10	Brass L63 [2]		40	2,5 20	15 15	4440 4438	-1,0 0,2	30,4 182	-3 -8
11	Alloy D16T [1]	100	25	5,0 20,0	15 15	6411 6411	0,19 -5,9	7,5 58,4	-4,7 34
12	Alloy D16T [2]		20	5,0 20,0	15 15	6409 6408	0,08 -0,92	10,3 132,6	-2,4 1,6
13	Copper M3 [1]	120	20	2,0 5,0	15 15	4650 4650	-32 -41	51 440	-2 74
14	Copper M3 [3]	120	20	2,0 5,0	15 15	4680 4680	3,7 3,0	22,0 223	-8,8 -30
15	Copper M3 [2]		10	2,0 5,0	15 15	4700 4700	-2,4 -3,0	49,9 420	7,5 40
16	Glass K8 [1]	60	20	5,0 30	10 10	5991 5993	-0,15 0,15	20,4 67,8	0,22 0,37
17	Quartz		25	5,0 30,0	10 10	5968 5968	0 <0,01	0,8 5,5	0 -0,18
18	Plexiglas		20	1,0 3,0	15 15	2750 2750	<0,1 <0,1	48 450	0,3 2
19	Alloy AMg5[1]		5 20	5 30	15 15	6384 6383	1 1	8,3 88,2	1,0 5

[1] sample in as-received condition, [2] flat section, as-received condition
[3] thermo-mechanical processing, [4] thermal processing.

In the experiments the plates with the plane-parallel working surfaces were used as samples in which the roughness of surfaces did not exceed 0,05 microns, planeness deviation on the basis of 50 mm was not more than 0,1 microns and misalignment was not more than 10^{-5} radian. The following materials (in as-received condition and thermo-mechanically processed) were used for samples: steel 3, steel 45, steel 40X13, steel X18H10T, brass L63, copper M3, alloy Д16T, glass K8, fused quartz of mark KB, organic glass, an aluminium alloy AMg5.

The received results have shown that for all samples heterogeneity in parameters C_L and α is characteristic. And for steel 40X13 and D16T in as-received condition, it is impossible to measure α with the error margin less than 50 % at the frequency range below 5-10 MHz. Heterogeneity of flat section samples (measurements were made perpendicularly to the rolling plane) is approximately 2-3 times less than heterogeneity of round samples of (measurements were made along the geometrical axis). Table 6 illustrates the heterogeneity estimation for all tested materials.

Conditions of thermal processing were: steel 40X13 – high annealing; steel X18H10T - normalization. Conditions of thermo-mechanical processing were: steel 40X13 - forging at 950^0C followed by hardening and tempering; copper M3 - forging at 200^0C followed by annealing at 350^0C and tempering during 2 hours.

From the table we can see that at the velocity C_L for all materials, except for steel X18H10T and copper M3, heterogeneity does not exceed 0,1 %. After thermal processing $\Delta C / C$ for steels 40X13

and X18H10T does not exceed 0,016 %. Thermo-mechanical processing of copper makes it possible to reduce heterogeneity to 0,08 %, and for steel 40X13 - to $1{,}7 \cdot 10^{-3}$ %. As one would expect, the least heterogeneity of metals in as-received condition is characteristic for steels 3 and steel 45.

Relative changes in attenuation factor reach 50 % and more, and at various frequencies they can have various signs (see the table, samples № 5÷7, et al.). Minimal relative changes α occur in steel 45 (among the metals in as-received condition) and the greatest effect for heterogeneity improvement is achieved by thermo-mechanical processing (samples № 5, 14).

Samples of glass, quartz and plexiglas (samples № 16, 17, 18) are the most homogeneous. In experiments it has been noted that for the samples with "optical" heterogeneity "acoustic" heterogeneity is also characteristic.

The measurements of samples made of the materials given in the table, but of other deliveries, have shown that a qualitative picture is the same, however from delivery to delivery the differences for α can reach 100 % and more (differences in the propagation velocity reach ± 20 m/s).

Thus, in fabricating standard samples to transfer the sizes of units of propagation parameters it is necessary to use either glass or metal after thermo-mechanical processing. The offered techniques of heterogeneity definition make it possible to define with high reliability the quality of initial materials and a finished product as well.

The presented results show the expediency of using the installation MAI-1 in case of the integrated study of acoustic parameters of various materials and their dependence on influencing factors (structure, chemical composition, temperature etc.). The major areas of MAI-1 application are: precision acoustic measurements in solid media, determination of elastic heterogeneity of a sample material, checking and certification of standard samples by attenuation factor of longitudinal US vibrations and by propagation velocity of longitudinal and shear acoustic waves.

Literature

1. Arkhipov V. I, Kondratjev A.I. Study of ultrasonic pulse propagation through a liquid layer. Defectoscopy. 1994. №4. P. 21-25

2. Bondarenko A.N., Drobot J.B., Kondratjev A.I. Precision acoustic measurements by optical and capacitance methods. - Vladivostok: FEB AS the USSR, 1990. 240 p.

3. Kondratjev A.I., Lugovoy V.A. Acoustic signal transducer for high precision measurements. Defectoscopy. 1990. №3. P.30-38.

4. Kondratjev A.I. Precision measurements of ultrasound velocity and attenuation in solid media. Acoustic Journal. 1990. V.36. №3. P. 470-476.

5. Kondratjev A.I. Precision methods and means for acoustic size measurements in solid media. – Khabarovsk: FESTU, 2006. 310 p.

Literature

1. Архипов В.И., Кондратьев А.И. Исследование прохождения ультразвукового импульса через слой жидкости. Дефектоскопия. 1994. №4. С. 21-25

2. Бондаренко А.Н., Дробот Ю.Б., Кондратьев А.И. Прецизионные акустические измерения оптическими и емкостными методами.- Владивосток: ДВО АН СССР, 1990. 240 с.

3. Кондратьев А.И., Луговой В.А. Датчик акустических сигналов для высокоточных измерений. Дефектоскопия. 1990. №3. С.30-38.

4. Кондратьев А.И. Прецизионные измерения скорости и затухания ультразвука в твердых средах. Акустический журнал. 1990. Т.36. №3. С. 470-476.

5. Кондратьев А.И. Прецизионные методы и средства измерения акустических величин твердых сред. В двух частях. – Хабаровск. Изд-во ДВГУПС, 2006. 310 с.